Research Article

An envelope shaping method for huge straight bevel gear

Peng Wang[1]

Received: 5 July 2019 / Accepted: 18 December 2019 / Published online: 23 December 2019

Abstract
An envelope shaping method of machining huge straight bevel gear is proposed in this paper. This method can achieve higher machining precision and efficiency. Firstly, the geometric characteristic of the tooth surface is analyzed. Then an envelope shaping principle is given. Based on this principle, the mathematical model of machine motion is built. In order to evaluate the machining precision, the enveloping error is derived. Calculation example shows that the enveloping precision can be controlled by adjusting enveloping times. On the whole, this paper lays a theoretical foundation for the machining technology of huge straight bevel gear.

Keywords Straight bevel gear · Envelope shaping method · Geometric characteristics · Enveloping precision

List of symbol

$S_1(x_1, y_1, z_1)$	The workpiece coordinate system
S	The generation surface of tooth surface
$\boldsymbol{S}(r, \varphi)$	The expression of tooth surface
$\boldsymbol{S}_r$	The tangent vector of tooth surface at the parameter r
$\boldsymbol{S}_\varphi$	The tangent vector of tooth surface at the parameter φ
$\boldsymbol{Q}(\varphi)$	The points on big end tooth profile of tooth surface
$\boldsymbol{W}(\varphi)$	The points on small end tooth profile of tooth surface
r	The direction parameter of the generatrix of cone
φ	The angle between the radius of initial position on the base cone bottom and the corresponding section radius on the base cone of the tangent of generation surface and base cone
δ_b	The base cone angle
δ_a	The tip angle
δ	The pitch cone angle
R	The cone distance
B	The tooth width of straight bevel gear
l_X	The movement distance at the X direction of machine
l_Y	The movement distance at the Y direction of machine
l_Z	The movement distance at the Z direction of machine
δ_n	The cone angle of cut-in point
k	The enveloping times
θ_a	The addendum angle
θ_f	The dedendum angle
h_a	The addendum
h_f	The dedendum
φ_n	The parameter value of the corresponding tooth profile equation at the cut-in point φ
θ	The angle between the projection of axis x_1 and the projection of workpiece axis in the projection plane

✉ Peng Wang, tjujxwp@126.com | [1]Tianjin Key Laboratory of High Speed Cutting and Precision Machining, Tianjin University of Technology and Education, Tianjin 300222, People's Republic of China.

θ_1	The angle between section radius of the start point of spherical involute on the base cone and section radius of the corresponding point of pitch cone on spherical involute
θ_2	The angle between section radius of the corresponding point of pitch cone on spherical involute and the projection of workpiece axis in the projection plane
$\boldsymbol{r}_1$	The direction vector of section radius of start point of spherical involute on the base cone at the workpiece coordinate system
$\boldsymbol{r}_2$	The direction vector of section radius of the corresponding point of pitch cone on spherical involute at the workpiece coordinate system
m	The modulus of workpiece
(x_t, y_t, z_t)	The coordinate of the any point on the projection plane at the workpiece coordinate system
$\Delta\theta_n$	The rotation angle of workpiece that the generatrix of every cut-in point of big end tooth profile rotate from the initial position of tooth profile generating to the position of located at the same line with the workpiece axis in the projection plane
$S_2(x_2, y_2, z_2)$	The aided coordinate system
$\overline{S}_n$	The chordal tooth thickness of big end
s_0	The parametric variable
λ_n	The angle between the tangent line of cut-in point on the projection of big end tooth profile and the projection of workpiece axis
γ	The nose angle of rhombus blade
β_n	The swing angle of cutter
H_X	The movement value of the X direction of machine in the process of transforming position
H_Y	The movement value of the Y direction of machine in the process of transforming position
N	The number of discrete point
$L_{Z(N)}$	The motion value of tool cutting edge movement to every discrete point with workpiece rotation at the direction of primary motion in the process of tooth forming
$L'_{Z(N)}$	The motion value of tool cutting edge movement to every discrete point if workpiece fixation at the direction of primary motion in the process of tooth forming
$r_{n(N)}$	The section radius of difference discrete point on the generatrix of every cut-in point
v_Z	The primary motion speed of machine
ω	The revolving speed of workpiece
$\beta_{n(N)}$	The swing angle of cutter with the primary motion
$\lambda_{n(N)}'$	The angle between the tangent line of spherical involute at every discrete point of the generatrix of cut-in point and the workpiece axis in the projection plane
$(q_x(\varphi), q_y(\varphi), q_z(\varphi))$	The point on the spherical involute of difference cone distance of theoretical tooth surface
η_n	The angle between the swing radius of the point of tool cutting edge tangent to tooth surface and the center line of cutter
l_n	The length of the contact point of tool cutting edge to tip point of cutter
l'_{max}	The swing radius of tip point of cutter
l'_n	The swing radius of the point of tool cutting edge tangent to theoretical tooth surface
$\boldsymbol{T}_n$	The direction vector of tool cutting edge
$\boldsymbol{F}_n$	The direction vector of the generatrix of cut-in point
(n_{nx}, n_{ny}, n_{nz})	The normal vector of planes formed by the tool cutting edge along the generatrix of cut-in point scanning
(A_i, B_i, C_i)	The direction vector of the intersection of adjacent planes
(x_0, y_0, z_0)	The common point of adjacent planes
d_j	The set of the minimum distance
μ	The enveloping precision

1 Introduction

The huge straight bevel gear whose diameter is larger than 3000 mm, is applied in more and more fields, such as power generation industry, shipping and mining

machinery etc. However, the manufacturing technology of this kind of gear cannot meet the efficiency requirement, because the current method is not available. Thus, it is necessary to development a suitable technology for huge straight bevel gear.

From the perspective of technological development continuity, the research results about the processing technology of straight bevel gear have certain reference value. The method of machining small and medium-sized straight bevel gear by milling machine was put forward in references [1, 2]. This method didn't need special cutter, such as tooth profile milling cutter, and special machine. But it was hard to achieve higher machining efficiency and machining precision. Therefore, it was not suitable for mass production. Aiming at straight bevel gears manufactured by dual interlocking circular cutters, Fuentes-Aznar et al. [3] did some research on the computerized generation and mesh simulation. The method of hot precision forging based on finite volume analysis was proposed in Ref. [4]. This method could promote machining efficiency and reduce production cost, but the mechanical properties and machining precision of the machined gear would be influenced. Qi et al. [5] proposed that due to high forming load and serious die wear, the large diameter straight bevel gear is seldom to manufacture by forging. So a new forming method is proposed to manufacture the straight bevel gear by a specific die with a flash and a boss. However, the small-end section and large-end section of tooth surface is incomplete filling. Aiming at this problem, the author proposed an optimization method. Shaikh and Jain [6] manufactured the straight bevel gears by ECH (electrochemical honing) process. The effect of finishing time and electrolyte composition on geometric accuracy and surface finish was studied. This research proves the capability of ECH to improve the quality of the bevel gears of any material hardness with high productivity. However, it doesn't make good business sense for huge straight bevel gear. A CNC EDM wire technology was used to machine huge straight bevel gear in Ref. [7].This processing method can achieve certain precision, and can be applied to machining huge straight bevel gear. But the machining efficiency was obviously low and the production cost was high. The method of machining straight bevel gear on the shaper machine was given in Ref. [8]. This method can meet the production requirement of huge straight bevel gear to some extent, but the defects of lower machining accuracy, poor universality of forming tool and higher production cost could not be overcame. The non-generating shaping method for huge straight bevel gear on the shaper was put forward in Ref. [9]. In the machining process, the cutter fed along the tooth profile tangent of the straight bevel gear's equivalent spur gear. Due to the deviation between the tooth profile of equivalent spur gear and the theoretical tooth profile, the machining error is unavoidable. A method of milling huge straight bevel gear by formed cutter was given in Ref. [10]. This method has poor universality and higher cutter manufacturing cost.

Aiming at above problems, an envelope shaping method on the CNC shaper is put forward. Firstly, the geometric characteristic of straight bevel gear tooth surface is analyzed. Then the envelope shaping principle of huge straight bevel gear is given. On this basis, the motion model to realize the machining principle is presented. Further, the motion model is used to study the relationship between the machining precision and the machining efficiency. Based on the above research results, a calculation example is given finally.

2 Geometric characteristics of straight bevel gear tooth surface

As we know, the tooth surface of straight bevel gear appears as an involute cone complying with the generation principle as shown in Fig. 1. Where, generation surface S is a circle plane whose center coincides with the base cone-apex O_1, and radius equals to the base cone distance R. The circle plane is tangent to the base cone. While the circle plane actives pure rolling on the base cone surface, the theoretical tooth surface is generated by the tangent line $A'A$. Here, the tooth profiles of big end and small end are both spherical involute [8]. It is clear that the tooth surface is a ruled surface [9–11]. As shown in Fig. 2, the tooth surface can be expressed as

$$\boldsymbol{S}(r,\varphi) = (1-r)\boldsymbol{W}(\varphi) + r\boldsymbol{Q}(\varphi) \tag{1}$$

where $\boldsymbol{Q}(\varphi)$ and $\boldsymbol{W}(\varphi)$ mean the points on the tooth profile of the big end and the small end respectively.

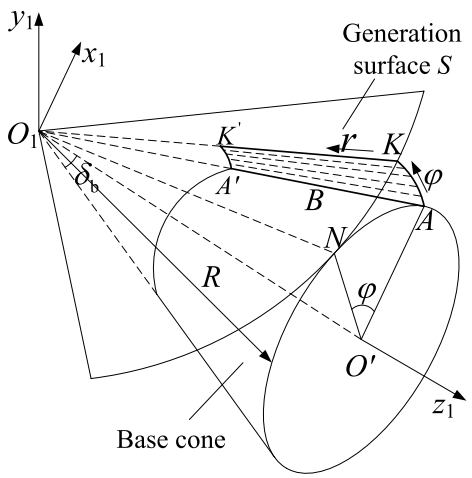

Fig. 1 Generation principle of straight bevel gear tooth surface

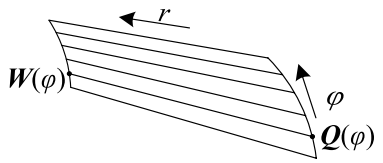

Fig. 2 Straight bevel gear tooth surface

The tangent vectors in the direction of the two parameters r and φ can be obtained through calculating partial derivative of Eq. (1), described respectively as:

$$\boldsymbol{S}_r = \frac{\partial \boldsymbol{S}(r,\varphi)}{\partial r} = \boldsymbol{Q}(\varphi) - \boldsymbol{W}(\varphi) \tag{2}$$

$$\boldsymbol{S}_\varphi = \frac{\partial \boldsymbol{S}(r,\varphi)}{\partial \varphi} = (1-r)\boldsymbol{W}'(\varphi) + r\boldsymbol{Q}'(\varphi) \tag{3}$$

It can be seen from Eq. (2) that the tangent vector of arbitrary point on a generatrix of the tooth surface keeps the same direction along r. As a result, the parameter r does not affect the concavity and convexity of the tooth surface. Therefore, the geometric characteristic of the tooth surface can be reflected by $\boldsymbol{S}_\varphi$.

$\boldsymbol{Q}'(\varphi)$ and $\boldsymbol{W}'(\varphi)$ mean respectively the tangent vector of the big and the small end in the direction φ of Eq. (3). In the coordinate system $S_1(x_1, y_1, z_1)$ of Fig. 1, the tooth profile of the big end and the small end can be expressed as:

$$\begin{cases} Q_x(\varphi) = R(\cos(\varphi \sin\delta_b)\sin\delta_b \cos\varphi + \sin(\varphi\sin\delta_b)\sin\varphi) \\ Q_y(\varphi) = R(\cos(\varphi \sin\delta_b)\sin\delta_b \sin\varphi - \sin(\varphi\sin\delta_b)\cos\varphi) \\ Q_z(\varphi) = R\cos(\varphi\sin\delta_b)\cos\delta_b \end{cases} \tag{4}$$

$$\begin{cases} W_x(\varphi) = (R-B)(\cos(\varphi \sin\delta_b)\sin\delta_b \cos\varphi + \sin(\varphi\sin\delta_b)\sin\varphi) \\ W_y(\varphi) = (R-B)(\cos(\varphi \sin\delta_b)\sin\delta_b \sin\varphi - \sin(\varphi\sin\delta_b)\cos\varphi) \\ W_z(\varphi) = (R-B)\cos(\varphi\sin\delta_b)\cos\delta_b \end{cases} \tag{5}$$

where $(Q_x(\varphi), Q_y(\varphi), Q_z(\varphi))$ means the coordinate of one point on the tooth profile of big end, $(W_x(\varphi), W_y(\varphi), W_z(\varphi))$ means the coordinate of one point on the tooth profile of small end, δ_b means the base cone angle, δ_a means the tip angle, R means the cone distance, B means the tooth width of straight bevel gear, and φ means the angle between $O'A$ and $O'N$ as shown in Fig. 1. According to the above calculation, φ can be arranged as:

$$0 \le \varphi \le \frac{\arccos\left(\frac{\cos\delta_a}{\cos\delta_b}\right)}{\sin\delta_b}$$

On the basis of Eqs. (4) and (5), the relationship between the tooth profile of big end and the tooth profile of small end can be expressed as:

$$\boldsymbol{W}(\varphi) = \frac{R-B}{R}\boldsymbol{Q}(\varphi) \tag{6}$$

When Eqs. (4) and (6) are substituted in Eq. (3), $\boldsymbol{S}_\varphi$ can be calculated as:

$$\boldsymbol{S}_\varphi = \left[(1-r)\frac{R-B}{R} + r\right]\boldsymbol{Q}'(\varphi) \tag{7}$$

where $Q'(\varphi) = (Q'_x(\varphi), Q'_y(\varphi), Q'_z(\varphi))$

It can be seen from Eq. (7) that $\boldsymbol{S}_\varphi$ is a space vector. As we know, the relationship between space vectors could be reflected by their projection. Obviously, $\boldsymbol{S}_\varphi$ is projected to the coordinate plane $x_1O_1y_1$, so the angle between vector projection and axis x_1 reflects the space change law of $\boldsymbol{S}_\varphi$. The included angle between the projection of $\boldsymbol{S}_\varphi$ and axis x_1 in plane $x_1O_1y_1$ can be expressed as

$$\cos\eta = \frac{Q'_x(\varphi)}{\sqrt{(Q'_x(\varphi))^2 + (Q'_y(\varphi))^2}} \tag{8}$$

To take the derivative of Eq. (8) by parameter φ, we get

$$\begin{aligned}(\cos\eta)' &= \frac{Q'_y(\varphi)[Q''_x(\varphi)Q'_y(\varphi) - Q'_x(\varphi)Q''_y(\varphi)]}{[(Q'_x(\varphi))^2 + (Q'_y(\varphi))^2]^{\frac{3}{2}}} \\ &= \frac{R^3\sin^3(\varphi\sin\delta_b)\sin\varphi(\sin^2\delta_b - 1)^3}{[(Q'_x(\varphi))^2 + (Q'_y(\varphi))^2]^{\frac{3}{2}}}\end{aligned} \tag{9}$$

In this equation, the denominator is greater than zero, and $\sin^2\delta_b < 1$ in the molecule in Eq. (9), so Eq. (8) is a monotone decreasing function. Therefore, the tooth surface of straight bevel gear is convex.

3 Envelope shaping principle and shaping method

Since the tooth surface is convex, it can be expressed approximately using the method of enveloping. As shown in Fig. 3, planes 1, 2 and 3 are tangent to tooth surface at the generatrix, and two adjacent planes intersect with each other. A multi-edge surface is formed by this way, which can be used to express approximately the tooth surface if the number of plane is enough.

In the above multi-edge surface, plane 1, 2 and 3 are formed by scanning of a cutter edge in the shaping process. In engineering practice, the rhombus blade is selected as the cutting edge.

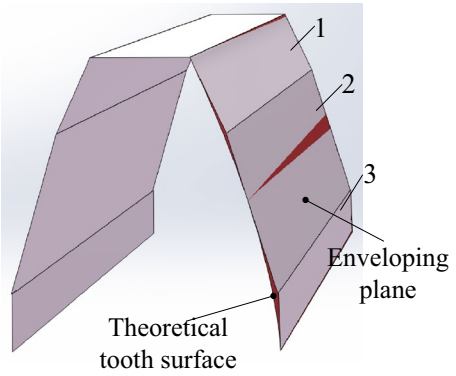

Fig. 3 Envelope tooth surface with planes

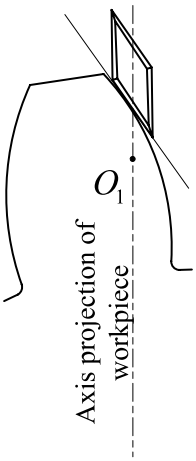

Fig. 5 Tooth profile projection of big end

Farther, the machining direction is set as from the big end to the small end, and along the pitch cone generatrix. According to the above settings, the relative position between the cutter and the workpiece is shown in Fig. 4.

In view that the weight of huge straight bevel gear is large, the workpiece should be always in a state of rotation to avoid position deviation caused by inertia. When the cutter begins to process, it needs to be considered further how to make the cutting edge tangent to the tooth profile of big end. According to the generation principle of tooth surface, the tooth profile of big end is space curve. To achieve this goal, this paper adopts the projection method. As shown in Fig. 4, the plane, which is parallel with the cutting edge plane and passes the conic node, is defined as projection plane. In this plane, the projection of cutting edge is tangent to the projection of tooth profile of big end. As shown in Fig. 5, when the generatrix of start-shaping position on the tooth profile of big end coincides with the axis of workpiece in the projection plane, the cutting edge should be tangent to the tooth profile of big end at this point by adjusting the position of cutter. The start-shaping position is named as cut-in point. Then, the cutting edge scans along the generatrix of cut-in point to form a plane. When the generatrix of the next cut-in point coincides with axis of workpiece in the projection plane, the cutting edge still should be tangent to the tooth profile at the cut-in point by adjusting the cutter. A multi-edge surface is formed by the cutter scanning one by one. And the dedendum is machined by the cutter-cusp according to the above machining method.

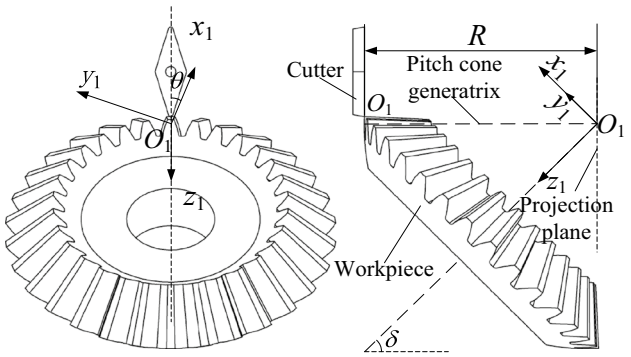

Fig. 4 Relative position between cutter and workpiece

4 Machine motion model

According to the above principle, the machine tool should include three kinds of motion. The first kind includes the motions of adjusting the machine before shaping. The second kind includes the motions of transforming the cut-in positions in the shaping process. And the last kind includes the motions of forming the tooth surface.

4.1 Machine adjustment motion model

The purpose of machine adjustment is to ensure that the generatrix of pitch cone is located at horizontal position and the workpiece axis is located at the same vertical plane with the direction of primary motion. The machine needs four motions to accomplish adjustment, including the angle adjustment of workpiece axis and the movements of machine along *X*, *Y*, *Z* direction.

Let the workpiece install on the rotary table, and the angle between the workpiece axis and ground is δ through adjusting the angle of rotary table. After adjustment, the workpiece and the cutter are located at the position shown in Fig. 4. The movement distances along *X*, *Y*, *Z* direction are respectively l_X, l_Y and l_Z.

4.2 Transformation model of cut-in position of tool cutting edge

The transformation of cut-in position of cutting edge requires four motions, including workpiece rotation, cutter swing, cutter movement along *X* direction and cutter

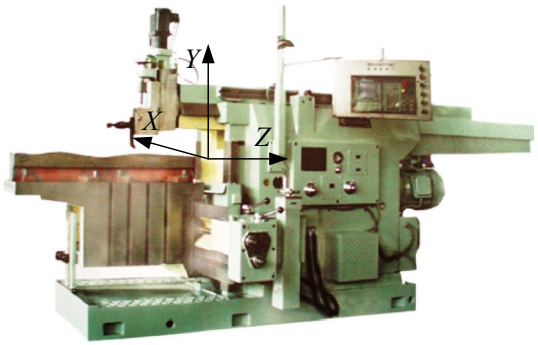

Fig. 6 Machine coordinate system

movement along *Y* direction (the machine coordinate system is shown in Fig. 6). All the above four motions are related to the position of cut-in point at the workpiece coordinate system (as shown in Fig. 4, the workpiece coordinate system is the coordinate system S_1), therefore, the position of cut-in point should be confirmed firstly at the workpiece coordinate system. The corresponding cone-apex angles of cut-in point are expressed as

$$\delta_n = \delta_a - n \cdot \frac{\theta_a + \theta_f}{k-1} \quad (n = 0, 1, 2, \ldots, k-1) \tag{10}$$

where $\delta_a = \delta + \theta_a$, $\theta_a = \arctan(h_a/R)$, $\theta_f = \arctan(h_f/R)$, δ is pitch cone angle, h_a is addendum, h_f is dedendum, k is the number of planes for enveloping tooth surface, and it is also named as the enveloping times.

The coordinate *z* of cut-in point at the workpiece coordinate system is obtained through the corresponding cone-apex angles of cut-in point δ_n as $z = R\cos\delta_n$. Let coordinate *z* substitute into Eq. (4), then φ_n (the corresponding parameter value of tooth profile equation at cut-in point φ) can be expressed as

$$\varphi_n = \frac{\arccos\left(\frac{\cos\delta_n}{\cos\delta_b}\right)}{\sin\delta_b} \tag{11}$$

Let the corresponding φ_n of cut-in point substitute into Eq. (4), the position of cut-in point at the workpiece coordinate system can be obtained.

The cutter swing angle and the cutter movement amount along *X* direction and *Y* direction are calculated in the projection plane. According to the above shaping method, the projection plane of the cutter and big end tooth profile is parallel with the cutting edge plane and pass the conic node. As shown in Fig. 4, the direction vector of the pitch cone generatrix is regarded as the normal vector of the projection plane. So, the coordinate *z* of the normal vector can be expressed as $R\cos\delta$ at the workpiece coordinate system. The component of the normal vector is $R\sin\delta$ at the coordinate plane $x_1O_1y_1$. The component coincides with the projection of workpiece axis at the projection plane, and θ is the angle between the axis x_1 and the projection of workpiece axis. According to the building process of the workpiece coordinate system, the axis x_1 is parallel with section radius of the start point of spherical involute on the base cone. As shown in Fig. 7, θ consists of angles θ_1 and θ_2. θ_1 means the angle between section radius of the start point of spherical involute on the base cone and section radius of the corresponding point of pitch cone on spherical involute. θ_2 means the angle between section radius of the corresponding point of pitch cone on spherical involute and the projection of workpiece axis in the projection plane.

θ_1 can be obtained by the direction vectors $\boldsymbol{r}_1$, $\boldsymbol{r}_2$ of the two section radius. The direction vector $\boldsymbol{r}_1$ can be expressed as

$$\boldsymbol{r}_1 = (R\sin\delta_b, 0, 0) \tag{12}$$

The direction vector $\boldsymbol{r}_2$ can be expressed as

$$\boldsymbol{r}_2 = (Q_x(\varphi), Q_y(\varphi), 0)\Big|_{\varphi=\frac{\arccos\frac{\cos\delta}{\cos\delta_b}}{\sin\delta_b}} \tag{13}$$

According to the calculation formula of vector angle, the angle θ_1 between $\boldsymbol{r}_1$ and $\boldsymbol{r}_2$ can be expressed as

$$\theta_1 = \arccos\left(\frac{\boldsymbol{r}_1 \cdot \boldsymbol{r}_2}{|\boldsymbol{r}_1||\boldsymbol{r}_2|}\right) = \arccos\left[\frac{Q_x(\varphi)\Big|_{\varphi=\frac{\arccos\frac{\cos\delta}{\cos\delta_b}}{\sin\delta_b}}}{R\sin\delta}\right] \tag{14}$$

Since the pitch cone tooth thickness of the big end of straight bevel gear is equal to the pitch circle tooth thickness of equivalent spur gear, θ_2 can be obtained with the help of this parameter. The pitch cone tooth thickness of

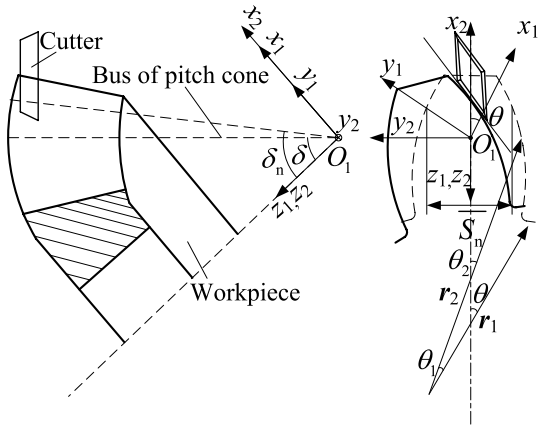

Fig. 7 The instant machining position of cutter and workpiece

big end is $0.5\pi m$ (m is modulus of big end), and the corresponding section radius is $R\sin\delta$. Therefore, θ_2 can be expressed as

$$\theta_2 = \frac{\pi m}{4R\sin\delta} \tag{15}$$

Through Eqs. (14) and (15), θ can be expressed as

$$\theta = \theta_1 + \theta_2 \tag{16}$$

So, the normal vector of the projection plane can be expressed as

$$n = (R\sin\delta\cos\theta, R\sin\delta\sin\theta, R\cos\delta) \tag{17}$$

Furthermore, the projection plane passes through the conic node (0, 0, 0), so the projection plane can be expressed as

$$x_t R\sin\delta\cos\theta + y_t R\sin\delta\sin\theta + z_t R\cos\delta = 0 \tag{18}$$

where (x_t, y_t, z_t) is the coordinate of one point on the projection plane at the workpiece coordinate system.

The projection curve of big end spherical involute at the workpiece coordinate system will be different if the workpiece rotates the different angle $\Delta\theta_n$. And $\Delta\theta_n$ can be obtained by the chordal tooth thickness of every cut-in point and the corresponding cone-apex angle. However, the chordal tooth thickness of straight bevel gear was usually calculated approximately using the tooth profile parameters of equivalent gear. The calculation method has theoretical error, which will affect the machining precision. For this reason, an accurately calculation method is put forward. Analyzing Fig. 7, the chordal tooth thickness of big end will be readily solved if the chordal tooth thickness of big end is parallel to a certain coordinate axis. Therefore, as shown in Fig. 7, an aided coordinate system $S_2(x_2, y_2, z_2)$ is built, whose origin point coincides with the conic node, and axis z_2 coincide with axis z_1. The angle between axis x_2 and axis x_1 is θ, and axis y_2 is located at the horizontal direction. Then the expression of spherical involute at the coordinate system S_2 can be obtained, and the double absolute value of the corresponding coordinate y is equal to the chordal tooth thickness of big end.

According to the principle of coordinate transformation, the spherical involute expressed by Eq. (4) at the workpiece coordinate system is transformed to the coordinate system S_2. The relationship of coordinate transformation is

$$\begin{bmatrix} x_2 \\ y_2 \\ z_2 \\ 1 \end{bmatrix} = \begin{bmatrix} \cos\theta & \sin\theta & 0 & 0 \\ -\sin\theta & \cos\theta & 0 & 0 \\ 0 & 0 & 1 & 0 \\ 0 & 0 & 0 & 1 \end{bmatrix} \cdot \begin{bmatrix} Q_x(\varphi) \\ Q_y(\varphi) \\ Q_z(\varphi) \\ 1 \end{bmatrix} \tag{19}$$

The chordal tooth thickness of big end can be expressed as

$$\overline{S_n} = 2|y_2| = 2\left|Q_y(\varphi_n)\cos\theta - Q_x(\varphi_n)\sin\theta\right| \tag{20}$$

Then, when the generatrix of every cut-in point is located at the same straight line with the workpiece axis in the projection plane, the rotating angle $\Delta\theta_n$ of workpiece can be expressed as

$$\Delta\theta_n = \arcsin\left(\frac{\overline{S_n}}{2R\sin\delta_n}\right) \tag{21}$$

According to Eqs. (21) and (4), the expression of big end tooth profile after workpiece rotation at the workpiece coordinate system is

$$\begin{bmatrix} P_x(\varphi) \\ P_y(\varphi) \\ P_z(\varphi) \\ 1 \end{bmatrix} = \begin{bmatrix} \cos\Delta\theta_n & \sin\Delta\theta_n & 0 & 0 \\ -\sin\Delta\theta_n & \cos\Delta\theta_n & 0 & 0 \\ 0 & 0 & 1 & 0 \\ 0 & 0 & 0 & 1 \end{bmatrix} \cdot \begin{bmatrix} Q_x(\varphi) \\ Q_y(\varphi) \\ Q_z(\varphi) \\ 1 \end{bmatrix} \tag{22}$$

The tooth profile expressed by Eq. (22) is projected to the projection plane expressed by Eq. (18). And the expression of the projection curve of big end tooth profile at the workpiece coordinate system after workpiece adjustment can be obtained according to the calculation method of Ref. [12]. The expression of projection curve is

$$\begin{cases} x_1(\varphi) = P_x(\varphi) - s_0 R\sin\delta\cos\theta \\ y_1(\varphi) = P_y(\varphi) - s_0 R\sin\delta\sin\theta \\ z_1(\varphi) = P_z(\varphi) - s_0 R\cos\delta \end{cases} \tag{23}$$

where s_0 is parametric variable, $s_0 = \frac{[P_x(\varphi)\cos\theta + P_y(\varphi)\sin\theta]\sin\delta + P_z(\varphi)\cos\delta}{R}$.

The cutting edge should be parallel with the tangent line of cut-in point in the projection plane. The swing angle of cutter is decided by the angle λ_n between the tangent line of big end tooth profile and the projection of workpiece axis, and nose angle γ of rhombus blade. According to cosine theorem, λ_n can be calculated by the tangent vector of the projection of big end tooth profile after workpiece rotation and the direction vector of workpiece axis projection.

Calculating the derivation of Eq. (23), so as to get the tangent vector is $\boldsymbol{T}_n = (x_1'(\varphi_n), y_1'(\varphi_n), z_1'(\varphi_n))$.` The angle λ_n between $\boldsymbol{T}_n$ and the unit vector, which passes the conic node as well as coincide with the projection of workpiece axis, can be expressed as

$$\lambda_n = \arccos\left\{\frac{[x_1'(\varphi_n)\cos\theta + y_1'(\varphi_n)\sin\theta]\cos\delta + z_1'(\varphi_n)\sin\delta}{\sqrt{x_1'(\varphi_n)^2 + y_1'(\varphi_n)^2 + z_1'(\varphi_n)^2}}\right\} \tag{24}$$

Then, according to Eq. (24), the swing angle β_n of cutter can be expressed as

$$\beta_n = \begin{cases} \lambda_n - \frac{\gamma}{2} & n = 0 \\ \lambda_n - \lambda_{n-1} & n > 0 \end{cases} \tag{25}$$

The center of blade will deviate from the former position after cutter swing. As shown in Fig. 8, the deviation distance of the blade center to the projection of workpiece axis is equal to the movement amount H_X along direction X. H_X can be expressed as

$$H_X = \begin{cases} l' \sin\beta_n & n = 0 \\ l'|\sin\beta_n - \sin\beta_{n-1}| & n > 0 \end{cases} \tag{26}$$

where l' is the swing radius of the center of rhombus blade.

The cutter movement amount H_Y after cutter swing is decided by distance H_1 from the blade center to the projection of conic node and distance H_2 from the blade center when the cutter is tangent to the projection of big end tooth profile to the projection of conic node. H_1 and H_2 can be expressed respectively as

$$H_1 = \begin{cases} H_n + l\cos\frac{\gamma}{2} + l'(1 - \cos\beta_n) & n = 0 \\ H_{n-1} + h_{n-1} - l'|\cos\beta_n - \cos\beta_{n-1}| & n > 0 \end{cases} \tag{27}$$

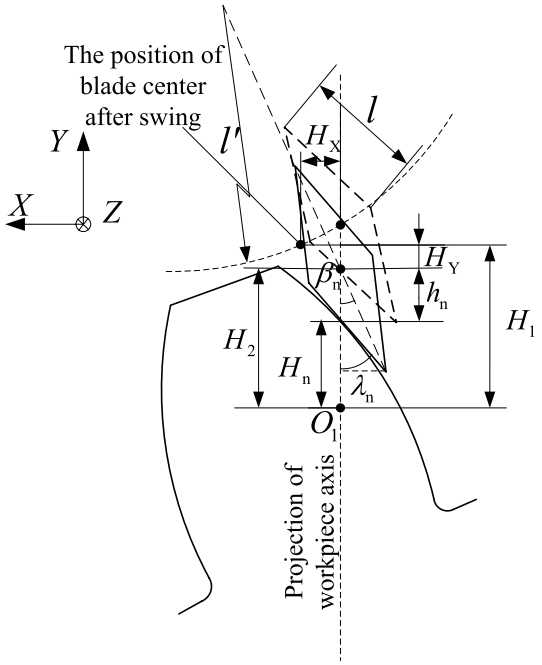

Fig. 8 Position of blade

$$H_2 = \begin{cases} H_n + h_n & \delta_n \geq \delta \\ H_n - h_n & \delta_n < \delta \end{cases} \tag{28}$$

where H_n is the projection length of the generatrix of cut-in point, $H_n = |R\sin(\delta_n - \delta)|$, $h_{n-1} = l\cos\frac{\gamma}{2}(\cos\beta_{n-1} - \sin\beta_{n-1}\tan^{-1}\lambda_{n-1})$, l is the cutting edge length of rhombus blade.

According to Eqs. (27) and (28), the machine movement amount along direction Y can be expressed as:

$$H_Y = \begin{cases} H_1 - H_2 & n \geq 0, \delta_n \geq \delta \\ H_1 + H_2 & n > 0, \delta_n < \delta \leq \delta_{n-1} \\ H_2 - H_1 & n > 0, \delta_{n-1} < \delta, \delta_n < \delta \end{cases} \tag{29}$$

4.3 Motion model of tooth surface forming

When the cutting edge is tangent to the projection of big end tooth profile at the cut-in point, the workpiece continues to rotate, and how to form the enveloping plane needs to be considered further. Due to the rotation of workpiece, the generatrix of cut-in point is not located at the same straight line with the workpiece axis in the projection plane. Therefore, the cutter needs to add one movement along direction X and direction Y respectively. It can be seen from Eq. (4), the different spherical involute equation can be obtained by changing the value of R. As shown in Fig. 9, the tangent line of projection curve of all spherical involutes at the same cut-in point are parallel, but the direction of tangent lines change also with workpiece rotation. In order to make the cutting edge still tangent to the theoretical tooth surface, the cutter needs to swing continuously with the primary motion of ram. To sum up, there are four tooth surface forming movements, the primary motion of ram, cutter swing, the cutter movement along direction X and the cutter movement along direction Y.

When the generatrix of cut-in point is located at the same straight line with the workpiece axis in the projection plane, the generatrix of cut-in point is dispersed as N points. With workpiece rotation, the position of discrete point changes,

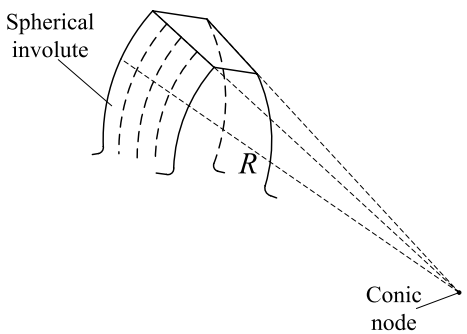

Fig. 9 Spherical involute

but the same discrete points of pre and post workpiece rotation are located at the same section arc of cone. The position of every discrete point after workpiece rotation are changed with the different revolving speed of workpiece, thus, the motion amount of cutter at the direction of primary motion is different, the relationship between the motion amount and the revolving speed is

$$L_{Z(N)} = L'_{Z(N)} + r_{n(N)}\left(1 - \cos\omega\frac{L_{Z(N)}}{v_Z}\right)\sin\delta \tag{30}$$

where $L_{Z(N)}$ is the motion amount at the direction of primary motion when the cutting edge moves to every discrete point with workpiece rotation. $L'_{Z(N)}$ is the motion amount at the direction of primary motion when the cutting edge move to every discrete point if the workpiece is fixed. $r_{n(N)}$ is the conic section radius of different discrete point on the generatrix of every cut-in point, $r_{n(N)} = \left[R - \frac{L'_{Z(N)}}{\cos(\delta_n - \delta)}\right]\sin\delta_n$. v_Z is the primary motion speed of machine. ω is the revolving speed of workpiece, and the range of ω can be obtained by Eq. (30).

After the motion amounts of the cutting edge at the direction of primary motion are decided, the next step is to determine the other three motion models.

(1) Cutter swing

The cutter swing is necessary to keep the cutting edge tangent to the tooth surface in the shaping process according to the envelope shaping principle. The swing angle is related to the cutter position and the angle between the tangent line of spherical involute at every discrete point on the generatrix of cut-in point and the workpiece axis in the projection plane. With workpiece rotation, the spherical involute corresponding to every cut-in point can be expressed as:

$$\begin{bmatrix} U_x(\varphi) \\ U_y(\varphi) \\ U_z(\varphi) \\ 1 \end{bmatrix} = \begin{bmatrix} \cos\Delta\theta'_{n(N)} & \sin\Delta\theta'_{n(N)} & 0 & 0 \\ -\sin\Delta\theta'_{n(N)} & \cos\Delta\theta'_{n(N)} & 0 & 0 \\ 0 & 0 & 1 & 0 \\ 0 & 0 & 0 & 1 \end{bmatrix} \cdot \begin{bmatrix} q_x(\varphi) \\ q_y(\varphi) \\ q_z(\varphi) \\ 1 \end{bmatrix} \tag{31}$$

where $\Delta\theta'_{n(N)} = \Delta\theta_n + \omega\frac{L_{Z(N)}}{v_Z}$, $(q_x(\varphi), q_y(\varphi), q_z(\varphi))$ is the point on the spherical involute corresponding to different cone distance, it can be expressed as

$$\begin{cases} q_x(\varphi) = \left(R - \dfrac{L'_{Z(N)}}{\cos(\delta_n - \delta)}\right)[\cos(\varphi\sin\delta_b)\sin\delta_b\cos\varphi + \sin(\varphi\sin\delta_b)\sin\varphi] \\ q_y(\varphi) = \left(R - \dfrac{L'_{Z(N)}}{\cos(\delta_n - \delta)}\right)[\cos(\varphi\sin\delta_b)\sin\delta_b\sin\varphi - \sin(\varphi\sin\delta_b)\cos\varphi]. \\ q_z(\varphi) = \left(R - \dfrac{L'_{Z(N)}}{\cos(\delta_n - \delta)}\right)\cos(\varphi\sin\delta_b)\cos\delta_b \end{cases}$$

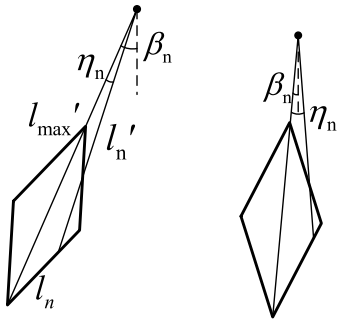

Fig. 10 Cutter swing

According to the method in Ref. [12], the projection curve of the above spherical involute can be expressed as:

$$\begin{cases} x_{tL_{Z(N)}} = U_x(\varphi) - s_1 R\sin\delta\cos\theta \\ y_{tL_{Z(N)}} = U_y(\varphi) - s_1 R\sin\delta\sin\theta \\ z_{tL_{Z(N)}} = U_z(\varphi) - s_1 R\cos\delta \end{cases} \tag{32}$$

where $s_1 = \frac{[U_x(\varphi)\cos\theta + U_y(\varphi)\sin\theta]\sin\delta + U_z(\varphi)\cos\delta}{R}$.

In accordance with Eq. (24), $\lambda'_{n(N)}$ can be expressed as:

$$\lambda_{n(N)} = \cos\left[\frac{(x'_{tL_{Z(N)}}\cos\theta + y'_{tL_{Z(N)}}\sin\theta)\cos\delta + z'_{tL_{Z(N)}}\sin\delta}{\sqrt{x'^2_{tL_{Z(N)}} + y'^2_{tL_{Z(N)}} + z'^2_{tL_{Z(N)}}}}\right] \tag{33}$$

Then, according to Eqs. (24) and (33), the cutter swing angle along with primary motion can be expressed as:

$$\beta_{n(N)} = \lambda'_{n(N)} - \lambda_n \tag{34}$$

(2) The motion along direction *Y*

Along with the workpiece rotation and the cutter swing, the straight line motion along direction *Y* is added to make the fixation point of the cutting edge keep along the generatrix of cut-in point in the shaping process. As shown in Fig. 10, the relationship between this motion and the primary motion is separated into two conditions:

When $\beta_n \geq \eta_n$, the relationship is:

$$L_{Y(N)} = \pm \left[L'_{Z(N)} \tan(\delta - \delta_n) - r_{n(N)} \left(1 - \cos\omega \frac{L_{Z(N)}}{v_Z} \right) \cos\delta \right] - l'_n [\cos(\beta_n - \eta_n) - \cos(\beta_n - \eta_n + \beta_{n(N)})] \quad (35)$$

where a positive value is picked when machining addendum to pitch cone, and a negative value is picked when machining pitch cone to dedendum. η_n is the angle between the swing radius of the tangent point on the cutting edge and the center line of cutter, $\eta_n = \arctan \frac{l_n \sin\frac{\gamma}{2}}{l'_{max} - l_n \cos\frac{\gamma}{2}}$. l_n is the length from the contact point on the cutting edge to the tip point of the cutter. l'_{max} is the swing radius of the tip point of the cutter. $l'_n$is the swing radius of the tangent point on the cutting edge with the theoretical tooth surface, $l'_n = \frac{l_n \sin\frac{\gamma}{2}}{\sin\eta_n}$.

When $\beta_n < \eta_n$, the relationship is

$$L_{Y(N)} = \pm \left[L'_{Z(N)} \tan(\delta - \delta_n) - r_{n(N)} \left(1 - \cos\omega \frac{L_{Z(N)}}{v_Z} \right) \cos\delta \right] + l'_n [\cos(\eta_n - \beta_n - \beta_{n(N)}) - \cos(\eta_n - \beta_n)] \quad (36)$$

(3) The motion along direction *X*

In order to make the cutting edge keep along the generatrix of cut-in point, the straight line motion along direction *X* is added. When $\beta_n \geq \eta_n$, the relationship between the motion along direction *X* and the primary motion of ram is

$$L_{X(N)} = r_{n(N)} \sin\omega \frac{L_{Z(N)}}{v_Z} + l'_n [\sin(\beta_n - \eta_n + \beta_{n(N)}) - \sin(\beta_n - \eta_n)] \quad (37)$$

When $\beta_n < \eta_n$, the relationship between the motion along direction *X* and the primary motion of ram is:

$$L_{X(N)} = r_{n(N)} \sin\omega \frac{L_{Z(N)}}{v_Z} + l'_n [\sin(\eta_n - \beta_n) - \sin(\eta_n - \beta_n - \beta_{n(N)})] \quad (38)$$

5 Enveloping precision controlling

The essence of the above forming principle is that the multi-edge surface approaches to the theoretical tooth surface. Obviously, the number k of planes forming multi-edge surface determines the enveloping precision. The maximum distance between the multi-edge surface and the theoretical tooth surface can show the enveloping precision. The intersection of adjacent planes needs to be obtained firstly for calculating the maximum value.

The mathematic model of planes formed by the cutting edge is obtained according to the knowledge that a plane is formed by two lines. The two lines are respectively the line of the cutting edge and the generatrix at the cut-in point. The direction vector of the cutting edge is $\boldsymbol{T}_n$ in the workpiece coordinate system. The coordinate of the cut-in point is $(P_x(\varphi_n), P_y(\varphi_n), P_z(\varphi_n))$ when the generatrix of the cut-in point is located at the same straight line with the workpiece axis in the projection plane, and the direction vector of the generatrix of cut-in point is $\boldsymbol{F}_n = (P_x(\varphi_n), P_y(\varphi_n), P_z(\varphi_n))$. Based on the above derivation, the planes scanned by the cutting edge can be obtained, expressed as:

$$n_{nx}(x - P_x(\varphi_n)) + n_{ny}(y - P_y(\varphi_n)) + n_{nz}(z - P_z(\varphi_n)) = 0 \quad (39)$$

where (n_{nx}, n_{ny}, n_{nz}) is the normal vector of the planes, and it can be obtained by multiplication cross between the vector $\boldsymbol{T}_n$ and the vector $\boldsymbol{F}_n$,

$$n_{nx} = y'_1(\varphi_n)P_z(\varphi_n) - z'_1(\varphi_n)P_y(\varphi_n),$$
$$n_{ny} = z'_1(\varphi_n)P_x(\varphi_n) - x'_1(\varphi_n)P_z(\varphi_n),$$
$$n_{nz} = x'_1(\varphi_n)P_y(\varphi_n) - y'_1(\varphi_n)P_x(\varphi_n)$$

According to Eq. (39), the intersection of adjacent planes can be expressed as

$$\frac{x - x_0}{A_i} = \frac{y - y_0}{B_i} = \frac{z - z_0}{C_i} \quad (40)$$

where (A_i, B_i, C_i) is the direction vector of the intersection, and it can obtain by multiplication cross of the normal vectors of the adjacent planes, where, $i = 0, 1, 2 \ldots k-2$ and $A_i = n_{iy}n_{(i+1)z} - n_{iz}n_{(i+1)y}$, $B_i = n_{iz}n_{(i+1)x} - n_{ix}n_{(i+1)z}$, $C_i = n_{ix}n_{(i+1)y} - n_{iy}n_{(i+1)x}$, (x_0, y_0, z_0) is the common point on the adjacent planes.

The intersection of adjacent planes expressed by Eq. (40) is dispersed into many points. The minimum distance between discrete point and theoretical tooth surface can be calculated using the grid algorithm in Ref. [13]. After calculation, a set of the minimum distance $d_j (j = 1,2,3\ldots)$ can be obtained, and the maximum value of the set is the enveloping precision μ

$$\mu = \max(\{d_1, d_2, \ldots, d_j\}) \quad (41)$$

The enveloping times k that meets the enveloping precision requirement can be obtained by the above calculation method.

Table 1 Gear parameters of huge straight bevel gear

Modulus, m	Pressure angle, α	Tooth number, Z	Tooth width, B	Pitch angle, δ	Pitch diameter, d
40	20	200	400	84°43′	8000

Table 2 δ_n, φ_n and $\overline{S_n}$ of every cut-in point

Cone-apex angle δ_n(°)	Parametric variable φ_n(°)	Chordal tooth thickness $\overline{S_n}$ (mm)
85°17′26″	81°48′05′	33.65
84°39′47″	79°50′47′	65.74
84°02′07″	77°52′34″	97.50

Table 3 Rotation angles of workpiece, swing angles of cutter and coordinates of cut-in point

Rotation angles of workpiece $\Delta\theta_n$ (°)	Swing angles of cutter β_n (°)	Coordinates of cut-in point (orkpiece coordinate system)
0°	2°38′22″	(3992.80, 292.00, 329.81)
13′48″	2°28′44″	(3991.20, 259.60, 373.64)
13′42″	2°15′47″	(3988.80, 227.60, 417.42)

Table 4 Tangent vector $\boldsymbol{T}_n$ of the projection of big end tooth profile and direction vector $\boldsymbol{F}_n$ of the generatrix at cut-in point

Tangent vector T_n of the projection of big end tooth profile	Direction vector $\boldsymbol{F}_n$ of the generatrix at cut-in point
(87.80, 514.90, − 1377.20)	(3992.80, 292.00, 329.81)
(89.60, 506.20, − 1367.50)	(3991.20, 259.60, 373.64)
(91.20, 496.30, − 1356.30)	(3988.80, 227.60, 417.42)

6 Calculation example

Taking a huge straight bevel gear as an example, the parameters are shown in Table 1. Aiming at this workpiece, the nose angle of rhombus blade is selected to be $\gamma = 35°$, and the enveloping precision requirement is 0.03 mm. The parameters of machine adjustment are calculated according to the above motion models, and then the minimum enveloping time is obtained by the method proposed in Sect. 5.

According to preliminary test, the enveloping time is initially selected to be k = 3. The cone-apex angle of every cut-in point is obtained using Eq. (10), and then the chordal tooth thickness at every cut-in point of the big end is calculated by Eqs. (10)–(20). The results are shown in Table 2.

The parameters in Table 2 are substituted into Eq. (21) to obtain the rotation angle $\Delta\theta_n$ of the workpiece. Then, according to Eq. (24), the angle λ_n is obtained using φ_n, $\Delta\theta_n$ and the projection equation of the tooth profile after workpiece rotation. The initial swing angle β_n is obtained by Eqs. (24) and (25).When the generatrix at the cut-in point is located at the same line with workpiece axis in the projection plane, the coordinate of cut-in point in the workpiece coordinate system is calculated by substituting φ_n into Eq. (22). The calculation results are shown in Table 3.

Substituting φ_n into $\boldsymbol{T}_n$, the direction vector $\boldsymbol{F}_n$ of the generatrix at the cut-in point can be obtained using the coordinates of cut-in point. The calculation results are shown in Table 4.

Substituting $\boldsymbol{T}_n$, $\boldsymbol{F}_n$ of Table 4 and coordinates of cut-in point in Table 3 into Eq. (39), the planes formed by the cutting edge can be expressed as

$$\begin{aligned} &\text{Plane 1}: x - 9.67y - 3.55z = 0\\ &\text{Plane 2}: x - 10.09y - 3.67z = 0\\ &\text{Plane 3}: x - 10.56y - 3.80z = 0. \end{aligned} \tag{42}$$

According to Eq. (40), the intersection between plane 1 and plane 2 and the intersection between plane 2 and plane 3 can be expressed respectively as

$$\begin{aligned} &\text{Intersection1}: \frac{x - 3978.10}{3.55} = \frac{y - 299.53}{-1.20} = \frac{z - 350.92}{4.26}\\ &\text{Intersection2}: \frac{x - 3975.00}{4.34} = \frac{y - 282.93}{-1.28} = \frac{z - 395.61}{4.70}. \end{aligned} \tag{43}$$

Substituting the parameters of the workpiece into Eq. (1), the theoretical tooth surface can be expressed as:

$$\boldsymbol{S}(r,\varphi) = (1-r)\boldsymbol{W}(\varphi) + r\boldsymbol{Q}(\varphi) \tag{44}$$

where the range of r is $0 < r < 1$, the range of φ is $77°52'34'' < \varphi < 81°48'05''$, $\boldsymbol{Q}(\varphi)$, $\boldsymbol{W}(\varphi)$ are respectively the tooth profile equation of the big end and the small end, and the expressions are

$$\begin{cases} Q_x(\varphi) = 3759\cos(0.94\varphi)\cos\varphi + 4017\sin(0.94\varphi)\sin\varphi\\ Q_y(\varphi) = 3759\cos(0.94\varphi)\sin\varphi - 4017\sin(0.94\varphi)\cos\varphi,\\ Q_z(\varphi) = 1417\cos(0.94\varphi) \end{cases}$$

$$\begin{cases} W_x(\varphi) = 3385\cos(0.94\varphi)\cos\varphi + 3617\sin(0.94\varphi)\sin\varphi\\ W_y(\varphi) = 3385\cos(0.94\varphi)\sin\varphi - 3617\sin(0.94\varphi)\cos\varphi\\ W_z(\varphi) = 1276\cos(0.94\varphi) \end{cases}$$

The intersections expressed by Eq. (43) are dispersed, and the distances of every discrete point to the theoretical tooth surface are calculated. A set of distances is obtained, and the maximum of the set is used to evaluate the enveloping precision. When the enveloping time k is 3, the enveloping precision μ is 0.033 mm, and μ is greater than the enveloping precision requirement 0.03 mm.

7 Discussion

As mentioned above, the enveloping precision can achieve 0.033 mm. This result is enough to meet the processing requirement of the huge straight bevel gear whose diameter is larger than 3000 mm. To further improve the accuracy, additional research has been done. According to the above calculation process, the relevant parameters and the enveloping precision are calculated again through increasing the enveloping times. The result shows that when the enveloping time k is 4, the enveloping precision μ is 0.009 mm, and this result can not only meet the enveloping precision requirement of this workpiece, but also reach the accuracy class in Ref. [1] which is for the smaller gear.

In terms of efficiency, the method proposed in this paper only needs 4 times of cutting for one tooth. Comparatively speaking, the CNC milling method proposed in Ref. [1] obviously has lower efficiency.

To sum up, this method can guarantee not only high machining precision but also higher machining efficiency.

8 Conclusions

1. An envelope shaping method for huge straight bevel gear is proposed in this paper. The research includes comprehensively the envelope shaping principle, shaping method, motion models of the machine and calculation method of enveloping precision. These results can be applied in practice to improve the production of huge straight bevel gear.
2. The calculation example shows that this method can guarantee not only high machining precision but also higher machining efficiency by means of adjusting enveloping times.
3. The research lays theoretical foundation for machine design to manufacture huge straight bevel gear.

Acknowledgements The author gratefully acknowledges the financial supports from Bureau-level Pre-research Project of Tianjin University of Technology and Education (No. KYQD1904).

Compliance with ethical standard

Conflict of interest The corresponding author states that there is no conflict of interest.

References

1. Kazumasa K, Kazuyoshi S (2009) Accuracy measurement and evaluation of straight bevel gear manufactured by end mill using CNC milling machine. J Mech Des. https://doi.org/10.1115/1.2988480
2. Cihan O, Ali I, Latif O (2005) An investigation on manufacturing of the straight bevel gear using end mill by CNC milling machine. J Manuf Sci Eng Trans ASME 127:503–511
3. Fuentes-Aznar A, Yague-Martinez E, Gonzalez-Perez I (2018) Computerized generation and gear mesh simulation of straight bevel gears manufactured by dual interlocking circular cutters. Mech Mach Theory 122:160–176
4. Saman K, Abdolrahman D, Taher A et al (2011) Design and manufacturing of a straight bevel gear in hot precision forging process using finite volume method and CAD/CAE technology. Int J Adv Manuf Technol 56:87–95
5. Qi Z, Wang X, Chen W (2019) A new forming method of straight bevel gear using a specific die with a flash. Int J Adv Manuf Technol 110(9–12):3167–3183
6. Shaikh Javed H, Jain NK (2015) Effect of finishing time and electrolyte composition on geometric accuracy and surface finish of straight bevel gears in ECH process. CIRP J Manuf Sci Technol 8:53–62
7. Xu CY (2009) The machine and technology of machining straight bevel gear using CNC wedm. Metal Manuf 16:53–55
8. Cao QL, Liu L, Qin T (1988) Processing of large straight bevel gear on the shaping machine. Mach Metal Cut 03:3
9. Qin QP, Zhang MY, Yu LF et al (1996) Non generating method shaping machining of large module straight bevel gear. Mach Manuf 1:11–13
10. Liu SH, Zhang Y (2003) The artifactitious milling about the large-size straight subulate gears. Coa Min Mach 2:45–46
11. Zhang C (2004) Mechanical Principle and Mechanical Design. Beijing, China
12. Li Y, Wang ML (2010) The calculation method of space curve projection equation on the general plane. Stud Coll Math 13:23–24
13. Xu RF, Chen ZT, Chen WY (2011) Grid algorithm for calculating the shortest distance from spatial point to free-form surface. Comput Integr Manuf Syst 17:95–100